Supporting Information for

Dual cross-linked cellulose based hydrogel films

Neethu Thomas, Saphia Moussaoui, Braulio Reyes-Suárez , Olivier Lafon, & G. N. Manjunatha Reddy*

University of Lille, CNRS, Centrale Lille Institut, Univ. Artois, UMR 8181−UCCS− Unité de Catalyse et Chimie du Solide, F-59000, Lille, France.

**Correspondence to be addressed: gnm.reddy@univ.lille.fr*

Contents

1. Preparation of gels

Materials: Carboxymethyl cellulose (CMC) was purchased from thermofisher scientific (analytical grade, degree of substitution: 0.9, average molecular weight: ~700 kDa and anhydrous citric acid, boric acid and Aluminum sulfate octadecahydrate ($Al_2(SO_4)_3 \cdot 18H_2O$) were procured from Sigma Aldrich (analytical grade) and were used as received.

Preparation of CMC-borate hydrogel. CMC was added to distilled water and stirred overnight to obtain a 4 wt% homogeneous solution. Variable concentration of boric acid (BA) (0.2, 0.3 and 0.5 equivalent) was added to CMC solution and stirred for 2 hours to obtain uniform dissolution. It was heated at 60 °C for 4 hours to obtain hydrogels. The obtained gels dissolved in water indicating cross linking was not achieved.

Preparation of CMC-epichlorohydrin hydrogel. A 2 wt% homogeneous solution of CMC powder was prepared by stirring adequate quantities of CMC in distilled water at room temperature overnight. Variable quantity of epichlorohydrin (ECH) (CMC anhydroglucose unit:ECH= 0.5:1, 1:1 and 2:1) was added and stirred at room temperature for 1 h to ensure uniform distribution. The mixture was kept in a water bath at 70 °C for 4.5 h to obtain CMC-ECH hydrogels.

Preparation of CA-Al and CMC-Al hydrogels. Aluminum sulphate was dissolved in distilled water to make a homogeneous solution. CMC powder (2 wt%) was slowly added to the aluminum solution with stirring. CMC:Al=3:1 equivalent was rationalized on the basis that one Al^{3+} ion could react with three carboxyl group. Nevertheless, the addition resulted in phase separation of hydrogel, which upon stirring at 70 °C resulted in separation and settling down of the gel part and water remained as a supernatant.

2. Synthesis procedure

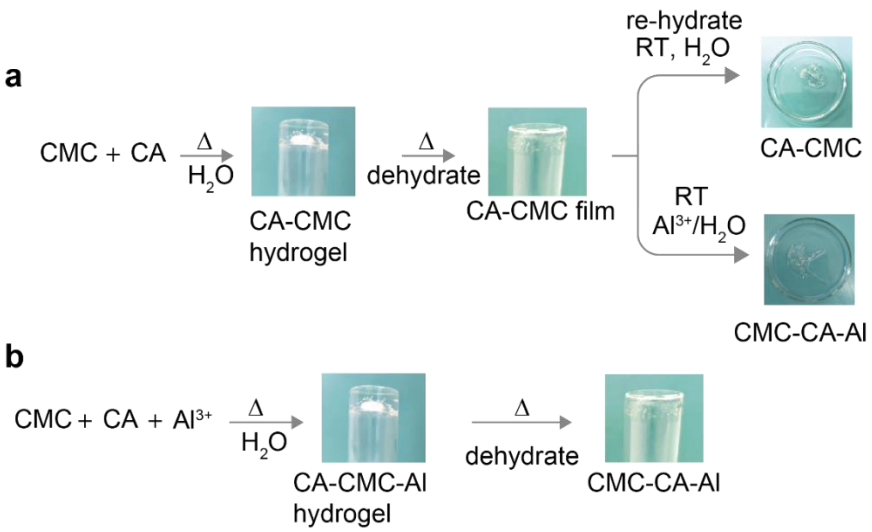

Figure S1. (a) Synthesis of mono cross-linked CMC-CA hydrogel and dual cross-linked CMC-CA-Al hydrogels obtained by sequencial addition of cross linkers (CA linked added first, followed by Al^{3+} ions). (b) Synthesis of dual cross-linked CMC-CA-Al hydrogels obtained by simultaneously adding CA and Al^{3+} cross linkers during the beginning of gelation process. Both methods provided stable hydrogels, though the populations of Al-complexes and their distributions are different for these gels.

3. CMC in water

Figure S2. CMC 2wt% (or above) in water, leading to a highly viscous, but poor gelation.

4. Gelation of CMC and boric acid

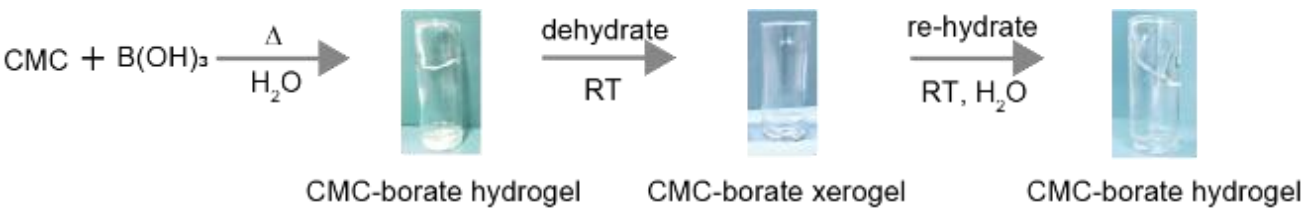

Figure S3. Gelation of CMC and BA. Photographs of reaction mixture and vial inversion test indicating flowing of the gel, and hence poor gelation. No hydrogel matrix/film formation occurred under the reaction conditions described.

5. Gelation of CMC and epichlorohydrin

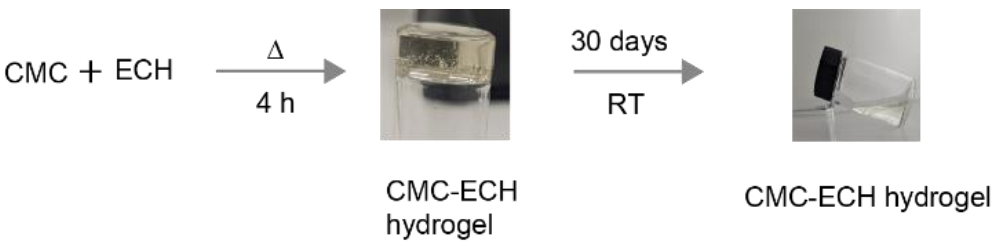

Figure S4. Gelation of CMC and epichlorohydrin (ECH) at 70 °C for ~4h. Photographs of reaction mixture and vial inversion test giving stable gel matrix. Dissolution of hydrogel was observed after 30 days at room temperature.

6. Impact of temperature on gelation of CMC and CA

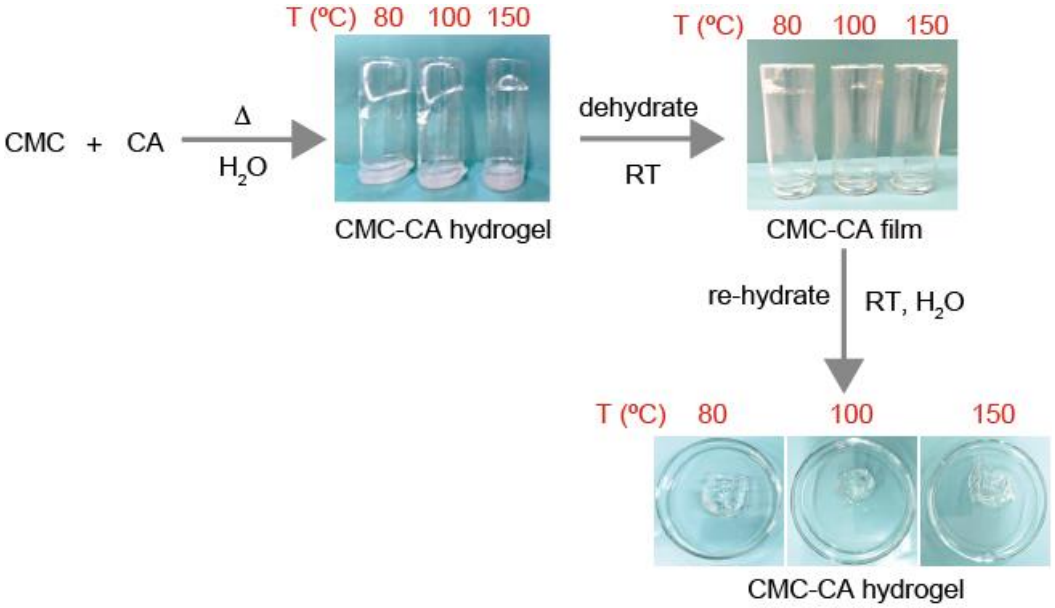

Figure S5. Gelation of CMCA and CA at 80, 100 and 150 °C. Photographs of reaction mixtures and vial inversion tests giving stable hydrogel films.

7. Impact of the CA concentration on gelation of CMC-CA

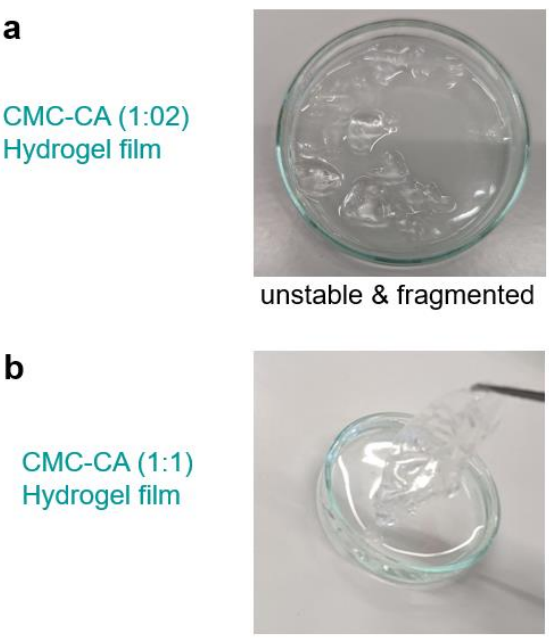

Figure S6. Impact of concentration of CA on gelation. Photographs of (a) CMC-CA (1:0.2) (b) CMC-CA (1:1) hydrogel films.

8. Proposed cross-linking reaction mechanism in CMC-CA

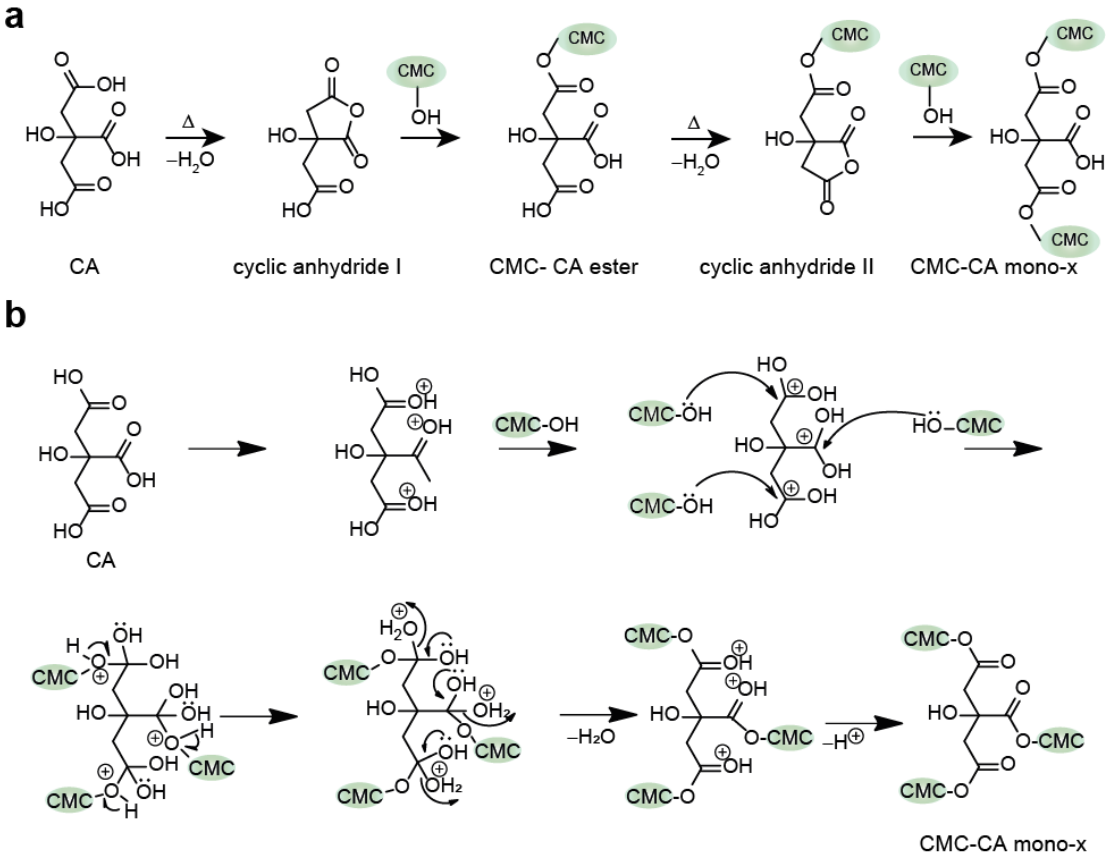

Figure S7. Plausible reaction mechanism for the formation of cross links between CA and CMC moieties.[6] (a) Mechanism involving CA cyclic anhydride and (b) involving tetrahedral intermediates, but likely to occur at reactive catalytic surfaces [7,8].

9. Solid state 1D ^{23}Na NMR of hydrogel film before and after soaking in water

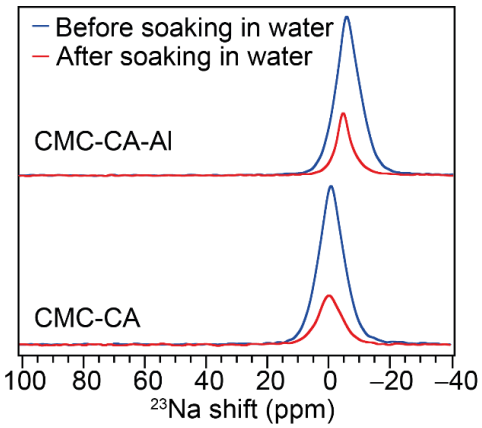

Figure S8. Solid-state 1D ^{23}Na MAS NMR spectra acquired at 18.8 T, 298 K, and 50 kHz MAS for dehydrated CMC-CA film before and after washing with water. The sodium content of CA-Al films are ~3 times lower after soaking in distilled water for an hour. The different ^{23}Na chemical shifts between CMC-CA (~0 ppm) and CMC-CA-Al (~5 ppm) are due to the different local chemical environments of Na cations in these materials.

10. Reaction of CMC and Al ions

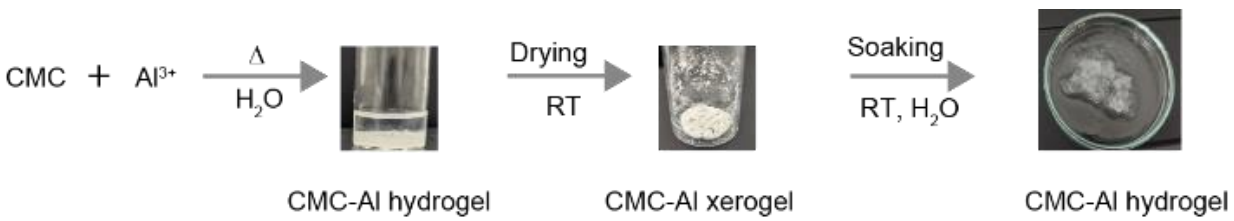

Figure S9. Schematic of a reaction between CMC and Al^{3+} ions in water together with photographs of solid-liquid phase separation in Al^{3+}/CMC binary mixture and obtained hydrogel matrix. No film formation occurred for the given concentrations of Al^{3+} and CMC (CMC:Al, 1:1 molar ratio).

11. CA-Al precipitate

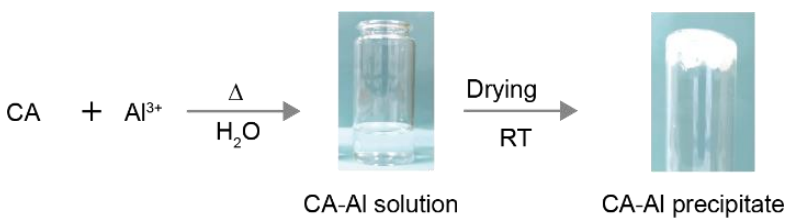

Figure S10. Schematic of a reaction between CA powder and Al^{3+} ions in water with photographs showing clear solution which formed a precipitate upon drying.

12. Thermal analysis of CMC and cellulose

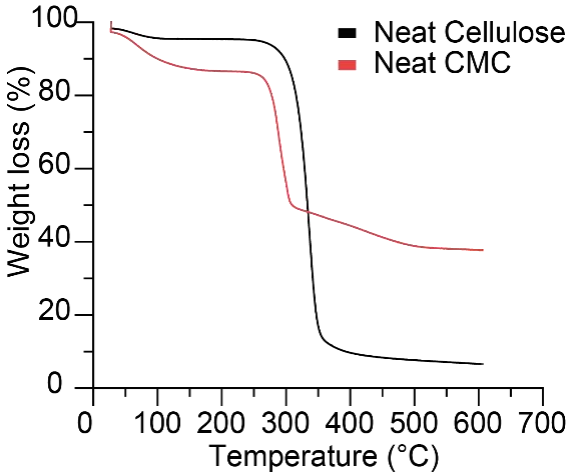

Figure S11. Thermal analysis of neat cellulose and neat CMC powders.

13. The 2D ^{1}H–^{1}H DQ-SQ correlation NMR spectrum of CMC

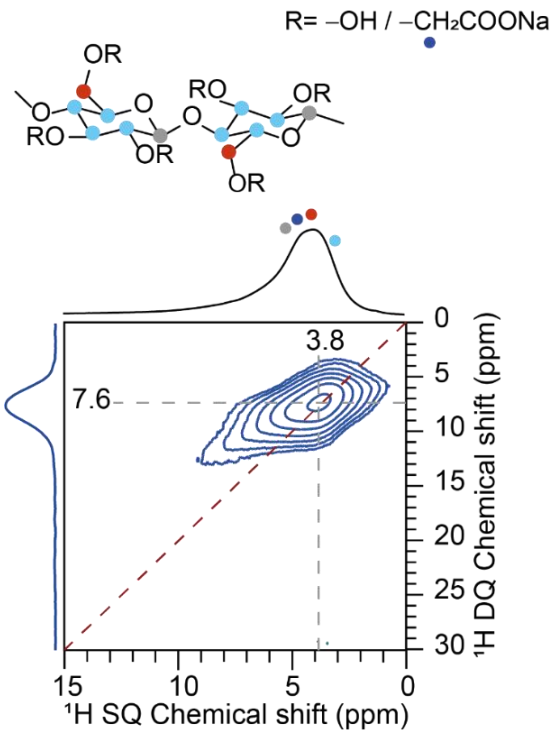

Figure S12. Solid-state 2D ^{1}H–^{1}H DQ-SQ correlation NMR spectrum of CMC acquired with DQ excitation time of 40 µs. Data was acquired at 21 T, (^{1}H = 900 MHz), 50 kHz MAS and 298 K.

14. Solid-state 1D ^{1}H NMR and packing interactions in CA

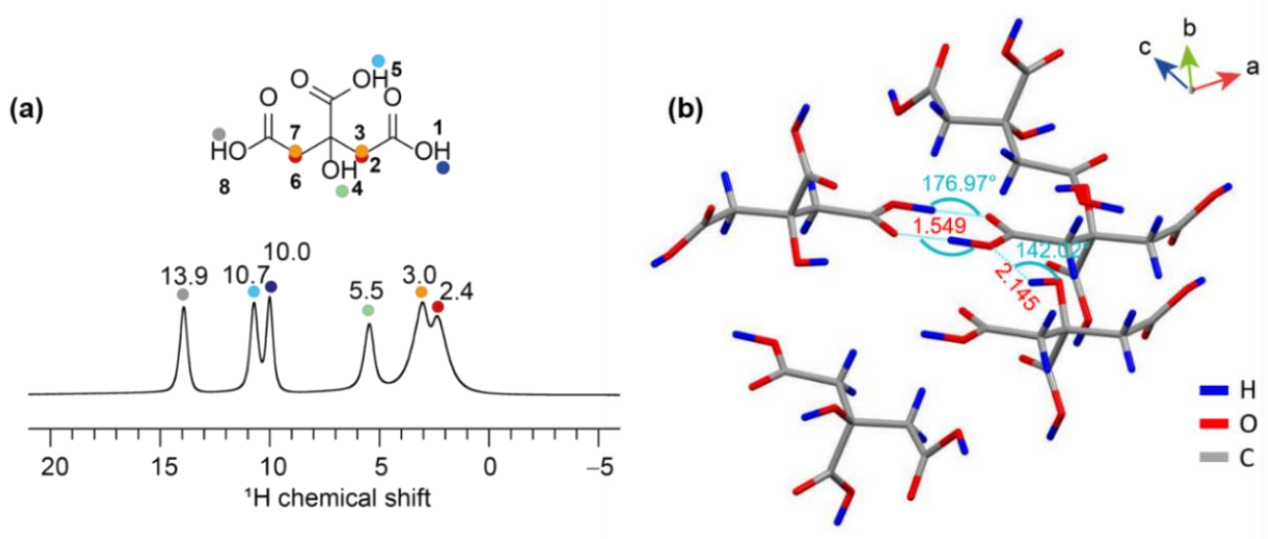

Figure S13. (a) Solid-state 1D ^{1}H MAS NMR spectra of CA powder acquired at 21.1 T, 298 K, and 50 kHz MAS, with color dots on peaks and in the molecular structure depicting the peak identification. (b) Crystal structure of CA obtained from Crystal Structure Database (CITRAC11).[9]

15. 2D ^{1}H–^{1}H spin-diffusion and DQ-SQ correlation NMR spectra of CA

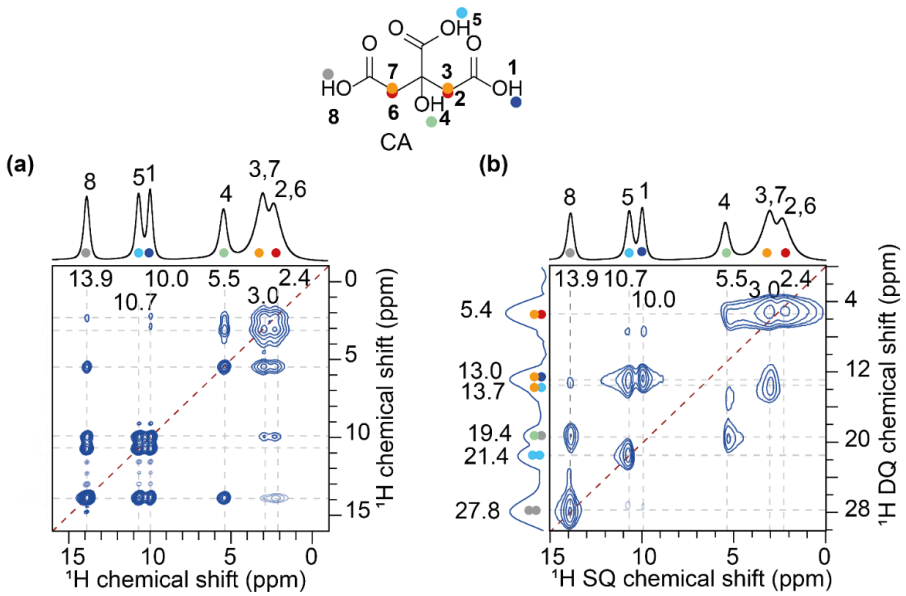

Figure S14. Solid-state **(a)** 2D ^{1}H-^{1}H Spin-Diffusion (SD) NMR of neat citric acid acquired using a SD time, t_{mix} = 500 ms. 1D ^{1}H MAS NMR spectrum of citric acid is given in the top horizontal axis. (b) 2D ^{1}H–^{1}H DQ-SQ correlation NMR spectrum of citric acid acquired with τ_{rcpl} = 40 µs recoupling time. In both cases, 1D ^{1}H MAS NMR spectrum of CA are presented on the top horizontal axes. All spectra were acquired at 21 T, (^{1}H = 900 MHz), 50 kHz MAS, and at 298 K.

16. Solid state 1D ^{1}H NMR spectra of CMC-CA xerogels

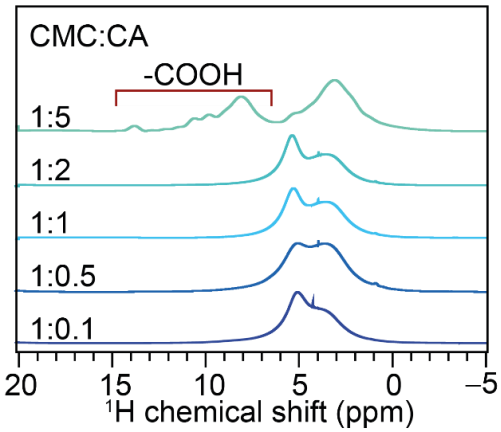

Figure S15. Solid-state 1D ^{1}H NMR spectra of CMC-CA xerogels with varying CA concentrations as indicated alongside the spectrum acquired at 28.2 T, 20 kHz MAS and 298 K. For CMC:CA=1:5 data was acquired at 18.8 T, 50 kHz and 298 K. High concentration of CA of 5 equiv. shows peaks in the range of 8-14 ppm, indicating the presence of unreacted –COOH moieties in CA.

17. Solid-state 1D ^{27}Al NMR spectra of CMC-CA-Al

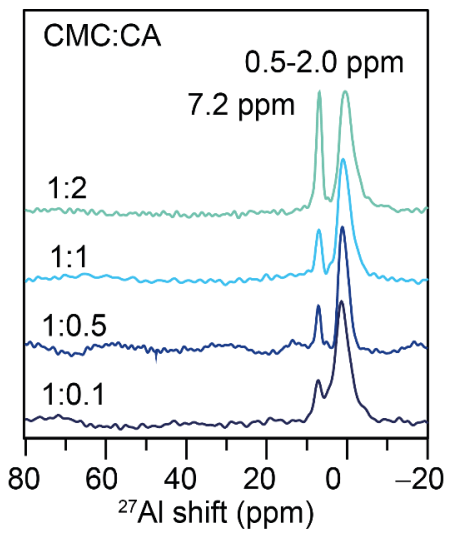

Figure S16. Solid-state 1D ^{27}Al NMR spectra of CMC-CA-Al xerogels with varying CA concentrations as indicated alongside the spectrum. Data were acquired at 28.2 T, 20 kHz MAS and at 298 K.

18. Solid-state 1D ^{27}Al NMR spectra of CMC-CA-Al xerogel and hydrogel

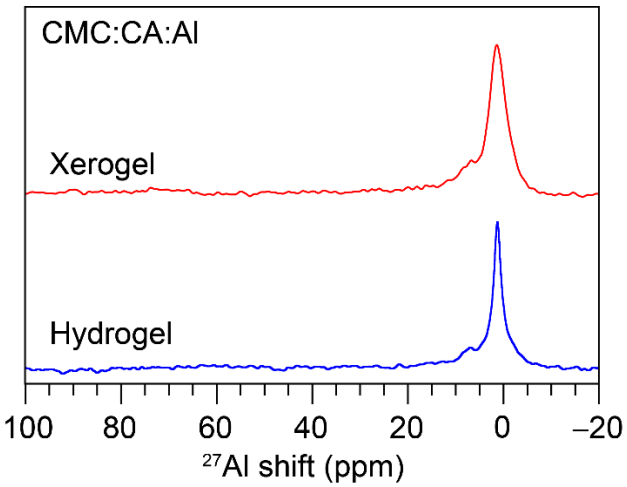

Figure S17. Solid-state 1D ^{27}Al MAS NMR spectra of CMC-CA-Al (CMC:CA=1:1 soaked in 0.1M Al^{3+} solution) xerogels (red) and hydrogel (blue). The spectrum for xerogel was acquired at 28.2 T (^{1}H = 1200.5 MHz, ^{27}Al = 312.9 MHz) with 50 kHz MAS. The spectrum for hydrogel was acquired at 18.8 T (^{1}H = 800.1 MHz and ^{27}Al = 208.4 MHz) with 8 kHz MAS.

A comparison of 1D ^{27}Al MAS NMR spectra of CMC-CA-Al xerogels and hydrogels (**Figure S17)** highlights both xerogel and hydrogel compositions exhibited identical ^{27}Al ssNMR spectra in terms chemical shifts and peak intensities. However, the narrower peaks in hydrogel compared to the dried powder could be attributed to the increased mobility (sol-gel environment) in hydrogels which leads to partially averaged anisotropic interactions such as chemical shift anisotropy, dipolar coupling and second-order quadrupolar interaction. This analysis indicates similar local coordination environments of Al^{3+} ions in hydrogels and xerogels.

19. Solid-state 1D ^{27}Al NMR spectra of hydrogels prepared using different synthesis methods.

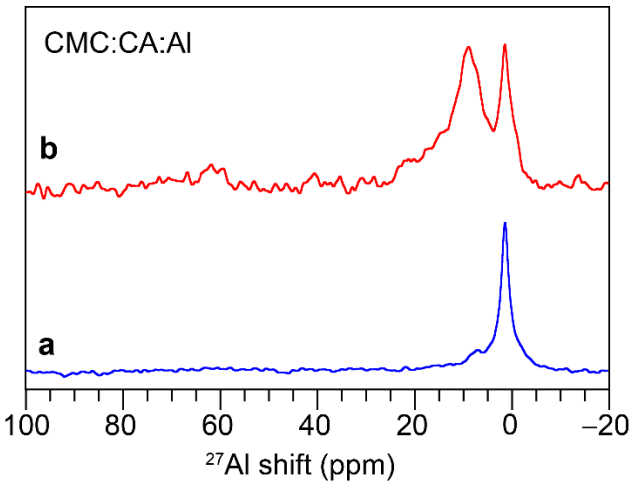

Figure S18. Solid-state 1D ^{27}Al MAS NMR spectra of CMC-CA-Al hydrogel prepared by (a) sequential addition of cross-linkers by soaking mono cross-linked CMC:CA=1:1 film in 0.1M Al^{3+} solution and (b) by simultaneously adding all precursors during the initial gelation process. Both spectra for were acquired at 18.8 T (^{1}H = 800.1 MHz and ^{27}Al = 208.4 MHz) with 8 kHz MAS.

After comparing the gelation methods (a) by sequential addition of cross linkers and (b) by simultaneous addition of cross linkers and heating up the sol-gel matrix, we obtained stable gels in both cases. Both methods produced stable gels, allowing flexibility in choosing the integration approach based on processing efficiency for a specific application. In method (a) we prepared hydrogels by covalently cross-linking CMC at 70 °C and immersing in Al^{3+} solution for aluminum ion uptake at room temperature to form additional cross links. In method (b) all ingredients are mixed and heated on a hot plate at 70 °C. Further, we characterized these hydrogels using gel-state ^{27}Al NMR spectroscopy **(Figure S18)**. Our results indicate that the relative populations are different for the hexacoordinated Al-aqua complexes (1-4 ppm) and the hexacoordinated Al-species (5-20 ppm) closely associated with the gel matrix, however, their local chemical environments are identical. Apparently, method (b) has more of the Al^{3+} ions closely associated with the gel matrix. We reasoned that this is due to high flexibility of the mono cross-linked CMC-CA-CMC moieties to accommodate more Al^{3+} ions into the gel matrix. This approach allowed us to explore how covalent cross-linking influenced ion absorption, demonstrating how ssNMR spectroscopy could be used as a tool to understand highly heterogeneous systems like hydrogels which are relevant in a broader context. This analysis highlights how different aluminum integration strategies influence the local chemical environments.

20. Solid-state 2D ^{27}Al-^{1}H correlation NMR spectrum

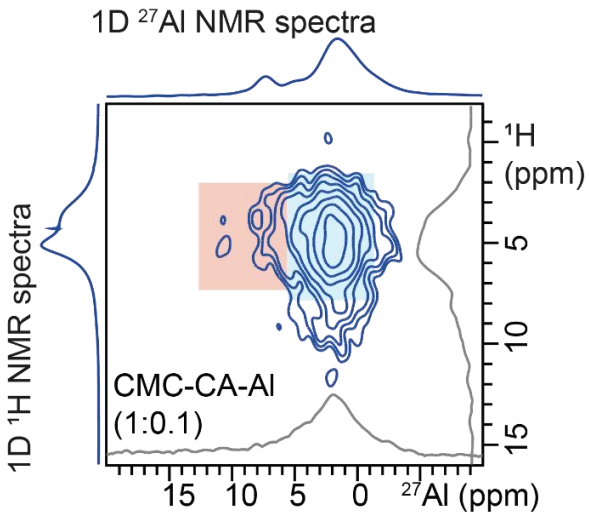

Figure S19. Solid-state 2D ^{27}Al-^{1}H correlation NMR spectrum plotted with the 1D ^{27}Al and ^{1}H sky-line projections shown in the inset for the CMC-CA-Al (CMC:CA, 1:0.5) xerogel. The corresponding 1D spectra are plotted on left vertical left and top-horizontal axes, respectively. Data was acquired with τ_{rcpl} = 500 µs at 28.2 T, 20 kHz MAS and 298 K.

21. Stability of dual cross-linked gels observed after 150 days

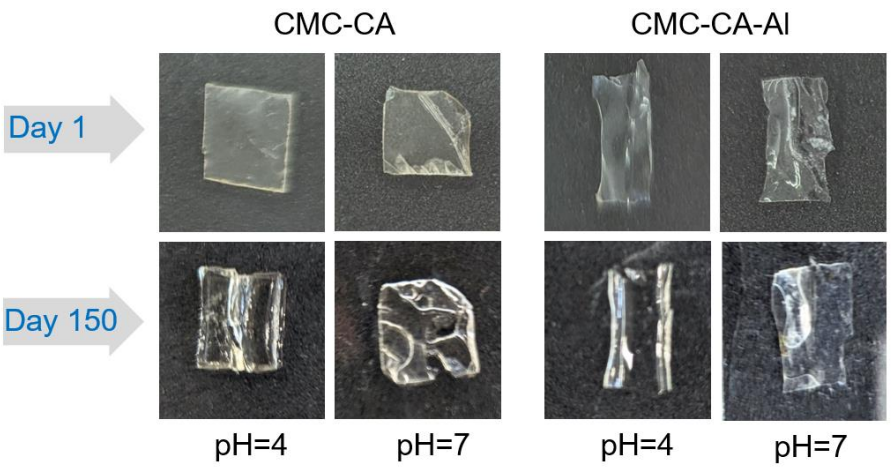

Figure S20. Photographs of CMC-CA and CMC-CA-Al dual cross-linked hydrogel films taken before and after immersing in aqueous solutions of pH = 4 and 7 for 150 days.

22. FT-IR transmittance plots of ion adsorbed hydrogel films

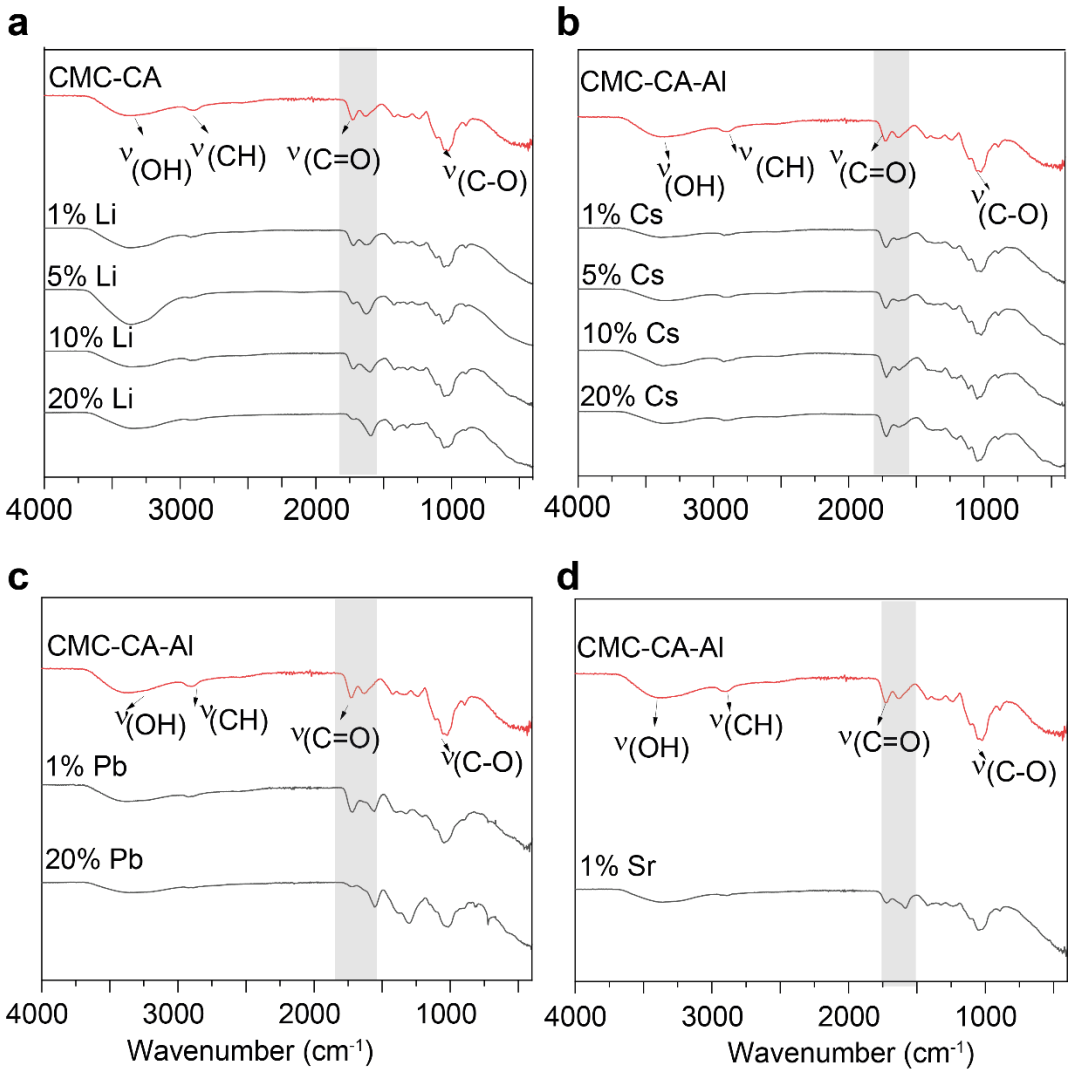

Figure S21. Solid-state attenuated FT-IR transmittance plots of (a) Li^{+}, (b) Cs^{+}, (c) Pb^{2+} and (d) Sr^{2+} adsorbed on hydrogel thin films.

23. Estimation of Cs^+ ion adsorption by CMC-CA-Al films

The total adsorption capacity of Cs^+ ions by CMC-CA-Al films was estimated by analyzing ^{133}Cs NMR spectra as a function of increasing concentration of Cs ions in water. These spectra were calibrated using an external reference (powdered CsCl, in which Cs at% = 78.9). To estimate the Cs^+ adsorption capacity of films single-pulse ^{133}Cs NMR spectra of Cs adsorbed CMC-CA-Al films were acquired at 18.8 T under identical conditions and compared with the standard CsCl of known mass. To ensure the quantitative nature of peaks corresponding to Cs^+ ions entrapped in gels, ^{133}Cs NMR spectra were recorded with respect to the relaxation delay of peaks in the range of 0-100 ppm (~1 s), although prolonged relaxation delay of other peaks resonating in the range 260-330 ppm can reach up to several hundreds of seconds. The standard CsCl had a high relaxation delay of 600 sec. Hence, S/N ratio of standard CsCl acquired with 4 scans was used to access the S/N ratio at the higher number of scans (see Experimental) at which the ^{133}Cs NMR spectra of Cs-adsorbed hydrogel films were recorded. The mass of Cs^+ ions in CsCl was used as an external calibration standard in order to estimate the amount of Cs^+ adsorbed on hydrogel films.

24. Solid state 1D ^{207}Pb NMR spectrum of Pb-adsorbed CMC-CA-Al hydrogel film

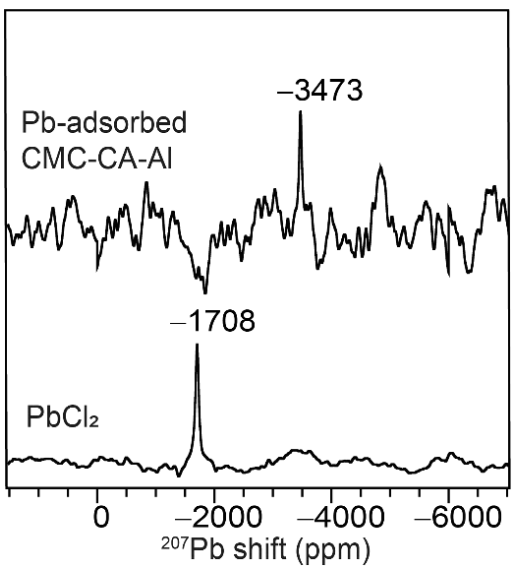

Figure S22. Solid state 1D ^{207}Pb NMR spectra of CsCl and CMC-CA-Al film after exposure to Pb^{2+} solution. All spectra were acquired at 18.8 T with 55 kHz MAS.

References

1 J. Trebosc, B. Hu, J.P. Amoureux, Z. Gan, *J. Magn. Reson.* 2007, **186**, 220-227.

2 A. Brinkmann and A. P. M. Kentgens, *J. Am. Chem. Soc.*, 2006, **128**, 14758–14759.

3 I. Schnell, A. Lupulescu, S. Hafner, D. E. Demco and H. W. Spiess, *J. Magn. Reson.*, 1998, **133**, 61–69.

4 G. N. M. Reddy, M. Malon, A. Marsh, Y. Nishiyama and S. P. Brown, *Anal. Chem.*, 2016, **88**, 11412–11419.

5 R. K. Harris, E. D. Becker, S. M. C. de Menezes, P. Granger, R. E. Hoffman and K. W. Zilm, *Pure Appl. Chem.*, 2008, **80**, 59–84.

6 G. F. de Lima, A. G. de Souza and D. dos S. Rosa, *Macromol. Symp.*, 2020, **394**, 1–9.

7 H. Yang, H. Song, H. Zhang, P. Chen and Z. Zhao, *J. Mol. Catal. A Chem.*, 2014, **381**, 54–60.

8 M. R. Altiokka and E. Ödeş, *Appl. Catal. A Gen.*, 2009, **362**, 115–120.

9 A.V.Churakov, *CCDC 635772 Exp. Cryst. Struct. Determ. 2007*.